

The strongest winds in tornadoes are very near the ground

Karen Kosiba ¹✉ & Joshua Wurman¹

Tornadoes contain some of the strongest winds on earth, causing death and damage when impacting man-made and natural objects, such as buildings and trees. Quantifying tornado winds near the surface is critical to characterizing tornado hazards. Direct measurements of tornado winds are rare and are usually obtained at least >100 m above the ground, well above building height, by proximate mobile radars. The representativeness of these mobile radar-obtained measurements to wind speeds closer to the surface is unknown. Here we analyze rare, low-level mobile radar observations of 73 different tornadoes to demonstrate that the strongest winds in tornadoes generally occur very near the ground. Therefore, even proximate radar measurements at >100 m above the ground usually substantially underestimate actual tornado wind intensity.

¹University of Illinois Champaign-Urbana, Urbana, IL, USA. ✉email: kakosiba@illinois.edu

Tornadoes contain some of the strongest winds on earth, causing death and damage when impacting man-made and natural objects, such as buildings and trees¹. Quantifying tornado windspeeds near the surface is critical to characterizing tornado hazards. In situ observations are exceedingly rare, and wind speeds are nearly always only inferred approximately, and likely with bias, from damage surveys^{2–4}. Occasionally, proximate mobile radars map tornado windspeeds, usually >100 m above the ground (AGL), well above typical building heights⁴. The representativeness of these measurements to windspeeds closer to the surface is unknown^{4–6}, severely limiting their interpretation and our understanding of near-surface tornado kinematics.

Here we show for the first time that the strongest supercell tornado windspeeds usually occur very near the ground and that radar observations at >100 m AGL usually are substantial underestimates of tornado intensity. Using rare, very low-level mobile radar observations of 73 different supercell tornadoes observed in the U.S. Great Plains we find that most such tornadoes exhibit a decrease in windspeed with increased altitude, with the strongest winds usually at the lowest observed levels. The median maximum tornado windspeed is 31% stronger at 15 m above the ground compared to radar measurements from higher altitudes. This is in contrast to the vertical distribution of the horizontal windspeeds in non-tornadic wind storms, in which windspeeds increase with height. Our results allow a more accurate quantification of tornado winds near the surface. We anticipate that these results will be used to update tornado hazard models⁶ and improve community risk assessments¹. Furthermore, knowledge of tornado windspeed profiles, and, in particular constraining the usual height of the maximum windspeed to <15 m AGL, provide a basis to refine numerical and theoretical wind models with observational constraints, increasing the understanding of near-surface tornado vortex kinematics and applicability of model results^{7–11}.

Results

Background. Damage-based inferences of near-surface tornado peak windspeeds using the Fujita² and Enhanced Fujita Scales³ exhibit significant errors, biases⁴ and uncertainties, and do not reveal the vertical wind speed profile of tornadoes since nearly all tornado-impacted structures are very near the surface. Proximate radars^{12–15} have measured tornado wind speeds up to $\sim 140 \text{ m s}^{-1}$, but these measurements usually are from >50 m above ground level (AGL), well above building heights. Wind speeds in nearly all atmospheric phenomena are stronger aloft compared to near the ground. Measurements from aloft can be reduced to infer windspeeds at heights relevant to human and structural impacts, e.g., 10 m AGL, using well established methods⁶. However, a tornado's winds might exhibit different behavior, the degree to which may depend on its structure and the turbulent characteristics of the boundary layer^{8,11}, so it has been unclear how to relate radar measurements of tornado winds at >50 m to near-surface values.

Mobile radars deploying proximately to tornadoes have been able to resolve tornado structures^{16–24} and, in rare instances, wind observations at multiple levels within 4–100 m above radar level (ARL) (Tornadoes observed by DOWs nearly always occur in very flat terrain, so ARL and AGL are nearly identical.) have been obtained^{25–27}. In rare, individual-case analyses of unknown generality, proximate radar data at multiple levels have revealed that wind speeds were strongest very near the ground^{27,28}, suggesting that even radar measurements from only several tens of meters ARL may be underestimates of true intensity.

Characterizing how these winds vary with height is necessary for understanding how winds observed aloft map to near-surface,

surface-, and structure-level winds. The Doppler on Wheels (DOWs)^{12,15} mobile radars have collected data in over 250 tornadoes spanning over three decades, and a broad range of intensities, vortex structures, and sizes²³, providing an expansive dataset through which near-surface tornado wind characteristics can be assessed (Fig. 1). In 73 of these tornadoes, DOW data were obtained at multiple levels, at least one of which was below 100 m ARL. These were used to construct vertical profiles of quasi-horizontal wind speed, allowing for the quantification of the general variation of tornado wind speeds as a function of height, and exploration of how these profiles vary from tornado to tornado, and with tornado intensity.

Doppler on wheels tornado windspeed profiles. The maximum wind speed at each observation height was extracted from the DOW data following standardized procedures⁴ (see methods section). Only time periods which had nearly contemporaneous measurements from at least two heights, at least one of which was <100 m ARL, were used for this analysis. At the time of peak tornado intensity, DOW-measured Doppler wind velocity (V_d) maps (Radars measure nearly instantaneous “Doppler Velocities” (V_d)²⁹. Radar-measured wind speeds in this analysis represent a very short period, $\ll 1$ s, spatially averaged, wind measurements, not average wind speeds, 1–3 s, or other averaging period wind gusts as measured by stationary anemometers. Critically, damage from tornadoes is believed to be caused by short period wind gusts^{2,3,6}) were used to determine tornado center locations, velocity difference across the tornado (DV), propagation velocity (V_p), calculate maximum ground-relative wind speeds in each radar slice through the tornado (V_g), and the maximum V_g observed below 100 m AGL (V_{gmax}). In order to compare tornadoes with different intensities, V_g were normalized by V_{gmax} to obtain $|V_g|$. Vertical profiles of $|V_g|$ and $d|V_g|/dz$, where z is height AGL/ARL, were extracted for 73 tornadoes.

Analysis of all $|V_g|$ profiles suggest that there is considerable variation in wind speed from the lowest observed levels to about 100 m ARL (Fig. 2A), and many of the profiles exhibit values near 1.0 near 100 m ARL. However, the height of the lowest observation level in each profile is different, ranging from 6 m to 98 m ARL, potentially skewing this result. Nearly all profiles that contained observations both at low levels (<15 m ARL) and at high levels (between 80–100 m ARL) exhibited the strongest winds near the lowest level, as indicated by the color coding of the profiles. Thus, the profiles containing data only near 100 m ARL likely did not sample the stronger wind speeds below, resulting in spuriously high normalized values aloft.

In order to mitigate the effects of this sampling bias, data were filtered to include only those profiles that began at low levels, <15 m ARL, resulting in profiles from nine tornadoes (Fig. 2B). There was considerable case-by-case variation in the profiles. Most of the profiles exhibit the strongest $|V_g|$ at the lowest levels. However, there are two exceptions, each associated with very weak tornadoes, with $DV < 45 \text{ m s}^{-1}$, typical of vortices described as “marginal tornadoes”¹⁵. These exhibit $|V_g|$ which increase with height in the lowest observed levels in the manner of non-tornadic windstorms. It is not clear if strengthening windspeeds with height is a property of marginal tornadoes since the 3rd profile associated with a marginal tornado does exhibit decreasing $|V_g|$ with height. Profiles from some slightly more intense tornadoes, with $50 < DV < 60 \text{ m s}^{-1}$, exhibit $|V_g|$ that weakens with increasing height.

Analysis of dV_g/dz allows examination of the vertical dependence of wind speeds and derivation of generalized vertical V_g profiles. Due to possible contamination of the lowest elevation radar scans by scattering from foliage, structures, and the ground^{29,30}, which can spuriously reduce V_d , $d|V_g|/dz$ was

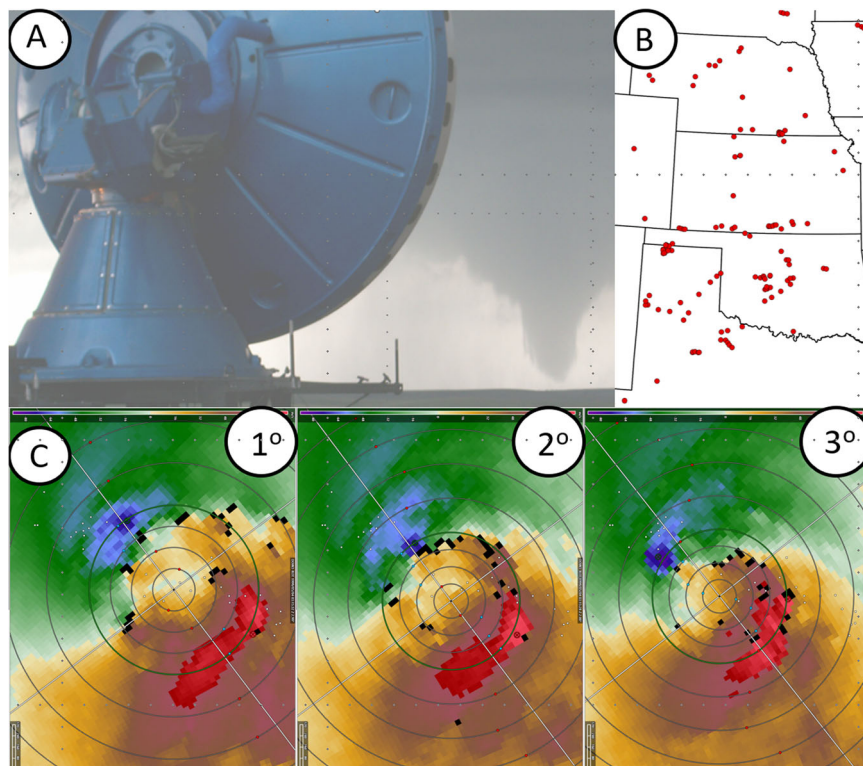


Fig. 1 DOWs observe tornado wind speeds. **A** DOW observing a tornado. **B** Map of locations of DOW-observed tornadoes 1995-2006. **C** Example of DOW V_d fields observed at three levels in a tornado. Blue/red = in/outbound. Note that the peak wind speed observed at each level is not necessarily immediately above the peak observed in the next lower level.

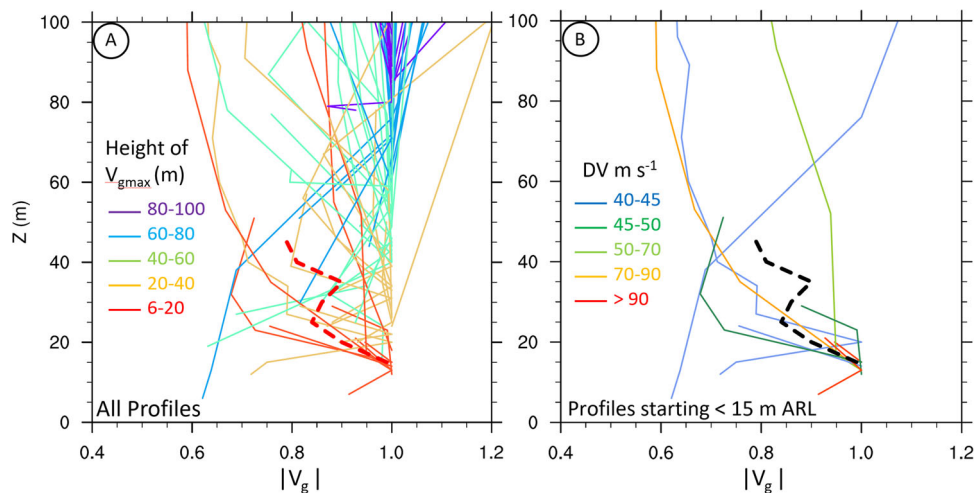


Fig. 2 Normalized windspeed $|V_g|$ profiles observed by DOWs. V_g normalized by V_{gmax} observed <100 m AGL. Dashed lines: median profile from the 2012 Russell, KS tornado²⁷. **A** All profiles containing observations <100 m ARL. Line colors are height of V_{gmax} in each profile. **B** Only profiles containing observations <15 m ARL. Line colors are DV observed at lowest level in each profile.

calculated using the 2nd and 3rd lowest height observations in each profile (Fig. 3). This revealed $d|V_g|/dz < 0$ from 15–90 m ARL. Median $d|V_g|/dz$ was approximately -0.005 (variance = 0.00007) from 17–35 m ARL, less negative (-0.002 to -0.0014 , variance = 0.00002) from 40–96 m ARL, and near zero (variance = 0.00001) above 96 m ARL. Integrating these median profile $\int d|V_g|/dz dz$ resulted in generalized DOW-observed tornado windspeed profiles (Fig. 4). These reveal that median $|V_g|$ decreases rapidly from 15 to 40 m AGL, then more slowly from 40 to 100 m AGL, and then very slowly from 100 to 140 m AGL.

Discussion

Theoretical, numerical, and laboratory modeling studies suggest that the strongest tangential winds occur near the top of the tornado boundary layer^{7,9}. Since boundary layer depth may vary as a function of surface roughness and/or tornado morphology, the height at which the maximum tangential winds occur is not expected to be the same for every tornado. Numerical modeling¹⁰ revealed the height of the maximum average tangential wind speed to range from ~30–70 m AGL, depending on model configuration, with average speed values 15% lower at 10 m AGL. Model analysis examined 10 m AGL wind gusts but only

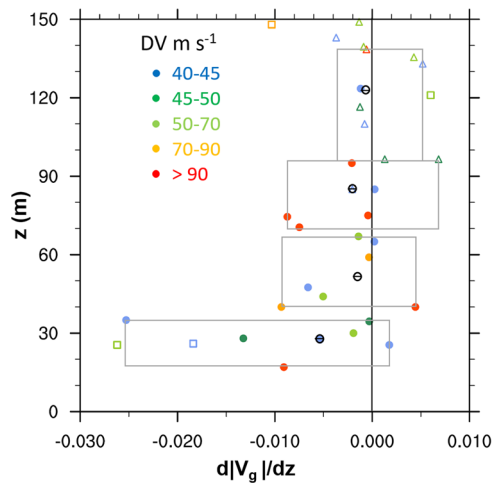


Fig. 3 Median and all samples of slope of DOW-observed tornado windspeeds $d|V_g|/dz$. Normalizations based on V_g observed at lowest level in each profile. Icon colors represent tornado vortex intensity, DV, at lowest level in each profile. Hollow triangles represent values with $dz > 50$ m. Hollow squares represent values with nearly identical radar beam elevations which are excluded from medians. Black circles are seven-sample medians of $d|V_g|/dz$ plotted at the mean z of the seven samples. Gray boxes outline $d|V_g|/dz$ and z spread of all values in each median.

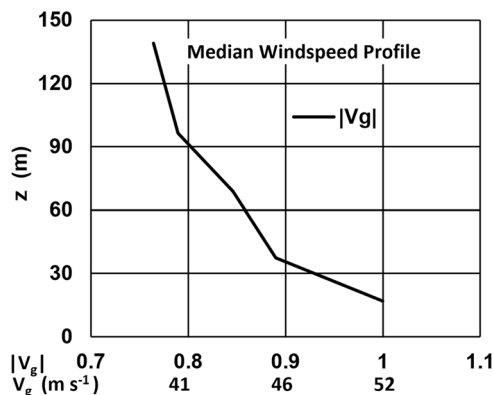


Fig. 4 DOW-observed tornado windspeed profile. Median $|V_g|$ profile based on DOW observations, and example of profile calculated using measured $V_g(140 \text{ m AGL}) = 40 \text{ m s}^{-1}$ implying $V_g(15 \text{ m AGL}) = 52 \text{ m s}^{-1}$.

calculated the average windspeeds at 30–70 m, and the vertical dependency of gusts is not discussed. Critically, since radars measure wind gusts, our current radar-based windspeed profile analysis directly addresses measured wind gusts as a function of height.

Because tornado winds are transient at any given point, damage resulting from tornadoes, and tornado intensity ratings, are associated with the effects of short period peak wind gusts on natural and man-made structures^{2,3,6}. Our results show that V_g at 15 m AGL average 31% stronger than V_g observed by radars at 100–140 m AGL, but with considerable case-by-case variation. The amount of underestimation depends on the minimum observation height. The profile in Fig. 4 can be used to calculate impactful near-surface (15 m AGL) tornado wind gusts from radar observations obtained aloft. For example, if radar indicated $V_g(140 \text{ m AGL}) = 40 \text{ m s}^{-1}$, low-level tornado V_g can be calculated as $V_g(15 \text{ m AGL}) = V_g(140 \text{ m AGL})/(1-0.235) = 52 \text{ m s}^{-1}$.

The wind speed profile reported in Fig. 4 is consistent with, but slightly steeper than, those previously reported^{27,28}. Critically, the

individual profiles, representing snapshots of V_g , reveal considerable variation among tornadoes and it has been demonstrated^{27,28} that there was considerable temporal variability of profiles during individual tornadoes. Therefore, using the current generalized results to extrapolate individual radar observations to infer the near-surface intensity of individual tornadoes should be conducted with caution. DOW observations at different levels are not truly simultaneous, and peak V_g in each radar scan are not necessarily immediately above peak V_g measured in immediately lower scans. Therefore, none of the profiles illustrated in Fig. 2 represent instantaneously-measured truly vertical profiles of V_g in precisely vertical columns.

These results have substantial implications for tornado hazard analysis and for validation and refinement of the wind-damage relationships that inform intensity determinations. However, we do not suggest that average structure-impacting tornado wind speeds are necessarily 31% ($1/(1-0.235) = 1.31$) stronger than measured by radars at 100–140 m ARL or those analyzed statistically⁴. Many, if not most, structures impacted by tornadoes suffer damage caused by winds at heights < 15 m AGL. There are not yet sufficient tornado wind speed observations from < 15 m ARL to extend the profile shown in Fig. 4 to the standard meteorological observation height of 10 m AGL. Residential structures common in tornado-prone areas typically extend from the ground to only about 3 m (single-story manufactured homes), 5 m (single-story house) or 8 m (two-story houses), with first stories centered at about 2 m AGL. Critically, the strength of winds in the 0–15 m AGL layer in the presence of man-made structures and trees are nearly impossible to sample by radar due to blockage from those same objects. Therefore, very near ground tornado V_g in built environments remain rarely sampled. Case study results suggest that maximum intensity winds may sometimes occur as low as 5 m AGL, but the radar data used in those studies were obtained over open land, not near or between houses and trees²⁷. Observations very near the ground by anemometers at 3 m AGL^{27,31} and at 1 m AGL³² suggest that peak wind gusts (V_g) in the 1–3 m AGL layer are less than or comparable to those measured by radars above the anemometers, but the impact of the built environment on these observations is unknown.

Methods

Navigation of DOW data. DOW radars have collected data in tornadoes since 1995. V_d data from several individual case studies, typically of intense or otherwise unusual tornadoes, have been navigated, processed, and analyzed in detail prior to this study^{14,16,18,21,23,27,28,31–35}, and a statistical analysis of ~100 tornadoes observed from 1995–2006 has been conducted⁴. In addition, dual-Doppler³⁶ and Ground-Based Velocity Track Display (GBVTD)^{35,37} analyses have been conducted for some tornadoes using navigated, processed and analyzed data. For this study, analyzed data from these previous studies, as well as from all additional tornadoes observed by DOWs during 2007–2009, are included.

Navigation of DOW data was achieved through a combination of Global Positioning System (GPS) locations and mapping of ground clutter targets. In most cases, data are from stationary leveled deployments when antenna pitch and roll were less than 0.2° as measured by precision bubble levels inside and near the antenna pedestals. During 1995–1999, and for a few cases during 2001–2005, data collected while DOWs were mobile were included. V_d were filtered using signal quality measures, such as signal-to-noise-ratio and returned power, and dealiased, as needed; data from non-meteorological targets were removed. No additional filtering was applied and V_d was analyzed in the native radar grid. When radar beam elevations are less than the radar beam width (B), a Gaussian-weighted correction raises the effective elevation angle such that they asymptote at 0.3° to account for terrain, tree, and structural blockage of the bottom portion of beams, with the effective elevation angle of a beam nominally pointing at 0.0° elevation being adjusted to 0.34° .

In this analysis, radar data are characterized by height ARL. When the ground height under a tornado is different than that under the DOW, AGL and ARL values will be different. This is rarely significant in the relatively flat terrain of the Plains, and at the close ranges over which most DOW tornado data are collected. This is especially true for the data included in this analysis, in which it was required that at least one observation be below 100 m ARL. Also, given the typically short ranges, non-linear and other anomalous propagation of radar beams is neglected, except

for the adjustment for blockage of the lower portion of ground-skimming beams discussed above.

The GURU software suite, developed by the Center for Severe Weather Research, was used to analyze several thousand cross-sections through candidate tornado vortices, most of which had been processed⁴, with tornadoes observed during 2007–2009 added. For each cross-section containing data in a candidate tornado vortex, the authors enter a first-guess center location and outline a ~2 km region enclosing the vortex. These are then used by GURU to calculate refined center locations, tornado diameter (X_d), and V_p . Automatically-determined center positions and X_d are reviewed by an expert team and refined as necessary. Sometimes this was required for complex vortices, containing sub-vortices or multiple wind speed maxima. In some cases, the determination of whether vortices were independent tornadoes or sub-vortices within multiple vortex mesocyclones^{16,18,23,34} was subjective. Centers, V_d fields, and V_p were used to automatically identify cross-sections containing V_{gmax} which were then used in this study.

Tornadoes spawned from quasi-linear convective systems and waterspouts were excluded from this study. Vortices were characterized as tornadoes when the maximum velocity difference across them (DV) was $\geq 40 \text{ m s}^{-1}$ within a $< 2 \text{ km}$ region^{4,23}, were associated with a mesocyclone and/or hook echo of a supercell thunderstorm and were not close to and/or associated with other tornadoes, thus excluding vortices along proximate gust fronts (“gustnadoes”) and nearby anticyclonic vortices²³. Vortices not observed below 100 m ARL were also rejected.

Calculation of Tornado metrics. The time of maximum intensity (defined as peak V_{gmax}) and various metrics of the wind field, including V_p , V_{gmax} , were calculated for each tornado. Some DOW-observed tornadoes may not have been observed at the time of maximum actual intensity. In some cases, V_p could not be determined from DOW measurements. This could occur due to irregular cross-section scheduling or the existence of only a single cross-section through the tornado. When needed, V_p was calculated from mesocyclone motion as measured by operational NWS WSR-88D radars. V_{gmax} at each observed level in a tornado was not required to be immediately above the next lower level V_{gmax} .

Adjustment for observation resolution and unobserved components of wind velocity. Following standardized procedures^{4,6} our analysis adjusts V_d for the effects of coarse spatial sampling and inferred unobserved V_{gmax} due to V_p . V_d are corrected for aspect ratio sampling errors^{4,38} by multiplying by $1/(1-0.48(B/X_d))$, where B is beamwidth, capped at 1.086, equivalent to what would be applied for $B/X_d > 6$, to arrive at a temporary product, adjusted velocity (V_{da}). V_d is a measure of only the towards/away component of the full wind velocity vector. For vortices propagating at any appreciable angle to the radar beams, the unobserved component of the wind velocity vector, $V_p \sin(\theta)$ where θ is the angle between V_p and the beam pointing angle, is significant. This is added to V_{da} to calculate V_{gmax} .

Eligible vertical profiles. Only data from tornadoes for which there were at least one DOW observation below 100 m ARL were included in this analysis. In some instances, observations were obtained at nearly identical levels, so that differences in height were much less than a radar beam width. Data in Fig. 4, for example, are flagged where the difference in radar beam elevation is $\ll B$, specifically 0.2° . Profiles were calculated for sweeps collected during a radar volume (usually a sequence of radar slices at increasing beam elevation) containing the time of peak V_{gmax} . However, in a few cases, there was no eligible profile in this volume (e.g., the volume was degenerate, containing only one slice). In these cases, the profile was extracted using the previous or following eligible volume, if the time of the low-level slice was within 60 s of the slice containing V_{gmax} .

Calculation of median statistics and profiles. Median $d|V_g|/dz$ statistics were calculated after eliminating values calculated from radar scans with differences in elevation of less than 0.2° or difference in height of 5 m or less, since these resulted in unreliable values of vertical derivatives since differences in V_d are likely dominated by temporal evolution. Medians were calculated from successively increasing mean height groups of seven $d|V_g|/dz$ values and plotted at the mean height of the values contributing to the medians. Profiles were calculated by piece-wise integrating the median $d|V_g|/dz$ profiles from 17–139 m AGL.

Data availability

Data are available via ftp transfer from the publicly accessible DOW Facility data archive by following instructions at the facility web site <http://dowfacility.atmos.illinois.edu> and/or emailing the lead author.

Received: 6 September 2022; Accepted: 15 February 2023;

Published online: 24 February 2023

References

- Ashley, W. S. & Strader, S. M. Recipe for disaster: How the dynamic ingredients of risk and exposure are changing the tornado disaster landscape. *Bull. Amer. Meteor. Soc.* **97**, 767–786 (2016).
- Fujita, T. T. “Proposed characterization of tornadoes and hurricanes by area and intensity” (SMRP Research Rep. 91, University of Chicago, 1971).
- Wind Science and Engineering Center, (WSEC), “A recommendation for an enhanced Fujita scale (EF-scale), revision 2” (WSEC, Texas Tech University, Lubbock, TX, (2006); <http://www.depts.ttu.edu/nwi/pubs/fscale/efscale.pdf>).
- Wurman, J., Kosiba, K., White, T. & Robinson, P. Supercell tornadoes are much stronger and wider than damage-based ratings indicate. *PNAS* **118**, e2021535118 (2021).
- American Society of Engineers (ASCE), Minimum design Loads for Buildings and other structures. *ASCE/SEI Standard 7-22* (2022).
- American Society of Engineers (ASCE), “Wind Speed Estimation in Tornadoes” in *Minimum Design Loads for Buildings and Other Structures*. *ASCE/SEI Standard 7-20* (ASCE draft 2022).
- Rotunno, R. The fluid dynamics of tornadoes. *Annu. Rev. Fluid Mech.* **45**, 59–84 (2013).
- Rotunno, R. A study in tornado-like vortex dynamics. *J. Atmos. Sci.* **36**, 140–155 (1979).
- Lewellen, W. S. Tornado Vortex Theory. In *The Tornado: Its Structure, Dynamics, Prediction, and Hazards* (eds. Church, C., Burgess D., Doswell C. & R. Davies-Jones, R.) (1993).
- Nolan, D. S., Dahl, D. S., Bryan, G. H. & Rotunno, R. Tornado vortex structure, intensity, and surface wind gusts in large-eddy simulations with fully developed turbulence. *J. Atmos. Sci.* **74**, 1573–1597 (2017).
- Lewellen, W. S., Lewellen, D. C. & Sykes, R. I. Large-eddy simulation of a tornado’s interaction with the surface. *J. Atmos. Sci.* **54**, 581–605 (1997).
- Wurman, J., Straka, J., Rasmussen, E., Randall, M. & Zahrai, A. Design and deployment of a portable, pencil-beam, pulsed, 3-cm Doppler radar. *J. Atmos. Oceanic Technol.* **14**, 1502–1512 (1997).
- Bluestein, H. B., French, M. M., PopStefanija, I., Bluth, R. T. & Knorr, J. B. A mobile, phased-array Doppler radar for the study of severe convective storms: The MWR-05XP. *Bull. Amer. Meteor. Soc.* **91**, 579–600 (2010).
- Pazmany, A. L., Mead, J. B., Bluestein, H. B., Snyder, J. C. & Houser, J. B. A mobile rapid-scanning X-band polarimetric (RaXPoL) doppler radar system. *J. Atmos. Oceanic Technol.* **30**, 1398–1413 (2013).
- Wurman, J. et al. The FARM (Flexible Array of Radars and Mesonets). *Bull. Amer. Meteor. Soc.* **102**, E1499–E1525 (2021).
- Wurman, J., Straka, J. M. & Rasmussen, E. M. Fine-scale Doppler radar observations of tornadoes. *Science* **272**, 1774–1777 (1996).
- Wurman, J. & Gill, S. Finescale radar observations of the Dimmitt, Texas (2 June 1995), tornado. *Mon. Wea. Rev.* **128**, 2135–2164 (2000).
- Wurman, J. The multiple-vortex structure of a tornado. *Weat. Forecast.* **17**, 473–505 (2002).
- Bluestein, H. B., Lee, W. C., Bell, M., Weiss, C. C. & Pazmany, A. L. Mobile Doppler radar observations of a tornado in a supercell near Bassett, Nebraska, on 5 June 1999. Part II: Tornado-vortex structure. *Mon. Wea. Rev.* **131**, 2968–2984 (2003).
- Bluestein, H. B., Weiss, C. C. & Pazmany, A. L. The vertical structure of a tornado near Happy, Texas, on 5 May 2002: High-resolution, mobile, W-band Doppler radar observations. *Mon. Wea. Rev.* **132**, 2325–2337 (2004).
- Kosiba, K., Trapp, R. J. & Wurman, J. An analysis of axisymmetric three-dimensional low-level wind field in a tornado using mobile radar observations. *Geophys. Res. Lett.* **35**, L5805 (2008).
- Weiss, C.C., Schroeder, J. L., Guynes, J., Skinner, P.S., & Beck, J. The TTUKa mobile Doppler radar: Coordinated radar and in situ measurements of supercell thunderstorms during Project VORTEX2. In *34th Conference on Radar Meteorology*, Williamsburg, VA. 11B.2. Boston: American Meteorological Society (Preprints) (2009).
- Wurman, J. & Kosiba, K. Finescale radar observations of tornado and mesocyclone structures. *Weather Forecast* **28**, 1157–1174 (2013).
- French, M. M., Bluestein, H. B., PopStefanija, I., Baldi, C. A. & Bluth, R. T. Mobile, phased-array, doppler radar observations of Tornadoes at X band. *Monthly Weather Review* **142**, 1010–1036 (2014).
- Alexander, C. R. & Wurman, J. The 30 May 1998 Spencer, South Dakota, storm. Part I: The structural evolution and environment of the tornadoes. *Mon. Weather Rev.* **133**, 72–97 (2005).
- Bluestein, H. B. et al. The structure of tornadoes near Attica, Kansas, on 12 May 2004: High-resolution, mobile, doppler radar observations. *Mon. Wea. Rev.* **135**, 475–506 (2007).
- Kosiba, K. A. & Wurman, J. The three-dimensional structure and evolution of a tornado boundary layer. *Weather Forecast.* **28**, 1552–1561 (2013).
- Wurman, J., Robinson, P., Alexander, C. & Richardson, Y. Low-level winds in tornadoes and potential catastrophic tornado impacts in urban areas. *Bull. Am. Meteorol. Soc.* **88**, 31–46 (2007).

29. Doviak R. J. & Zrnic, D. S. *Doppler Radar and Weather Observations*. Dover Publications, Minneola, NY. 562 pp. (1984).
30. Snyder, J. C. & Bluestein, H. B. Some considerations for the use of high-resolution mobile radar data in tornado intensity determination. *Wea. Forecasting* **29**, 799–827 (2014).
31. Wurman, J., Kosiba, K. & Robinson, P. In situ, Doppler radar, and video observations of the interior structure of a tornado and the wind–damage relationship. *Bull. Am. Meteorol. Soc.* **94**, 835–846 (2013).
32. Kosiba, K. A. & Wurman, J. The TWIRL (Tornado Winds from In-situ and Radars at Low-levels) Project. *28th Conf. on Severe Local Storms*, Portland, OR, Amer. Meteor. Soc., 4.2, <https://ams.confex.com/ams/28SLS/webprogram/Paper302011.html> (2016).
33. Wurman, J. & Alexander, C. R. The 30 May, 1998 Spencer, South Dakota, storm. Part II: Comparison of observed damage and radar-derived winds in the tornadoes. *Mon. Weather Rev.* **133**, 97–119 (2005).
34. Wurman, J., Kosiba, K. A., Robinson, P. & Marshall, T. The role of multiple vortex tornado structure in causing storm researcher fatalities. *Bull. Am. Meteorol. Soc.* **95**, 31–45 (2014).
35. Kosiba, K. & Wurman, J. The three-dimensional axisymmetric wind field structure of the Spencer, South Dakota, 1998 Tornado. *J. Atmos. Sci.* **67**, 3074–3083 (2010).
36. Kosiba, K. et al. Genesis of the Goshen County, Wyoming, Tornado on 5 June 2009 during VORTEX2. *Mon. Wea. Rev.* **141**, 1157–1181 (2013).
37. Lee, W. C. & Wurman, J. Diagnosed three-dimensional axisymmetric structure of the Mulhall tornado on 3 May 1999. *J. Atmos. Sci.* **62**, 2373–2393 (2005).
38. Burgess, D. W., Donaldson, R. J. Jr., & Desrochers, P. R. “Tornado detection and warning by radar” in *The Tornado: Its Structure, Dynamics, Prediction and Hazards*, *Geophys. Monogr.*, Vol. 79, pp. 203–221 (Amer. Geophys Union, 1993).

Acknowledgements

We thank Paul Robinson and Trevor White for assistance with analysis and figures, Maiana Hanshaw for reviewing the manuscript, and the many DOW crew. Analysis and preparation of manuscript supported by the University of Illinois. Support for data collection and instrument development from the National Science Foundation.

Author contributions

K. K. contributed: Analysis and Writing. J. W. contributed: Analysis and Writing.

Competing interests

The authors declare no competing interests.

Additional information

Correspondence and requests for materials should be addressed to Karen Kosiba.

Peer review information : Communications Earth & Environment thanks Donald Burgess, Jeffrey Snyder and James LaDue for their contribution to the peer review of this work. Primary Handling Editors: Joy Merwin Monteiro, Joe Aslin and Clare Davis.

Reprints and permission information is available at <http://www.nature.com/reprints>

Publisher’s note Springer Nature remains neutral with regard to jurisdictional claims in published maps and institutional affiliations.



Open Access This article is licensed under a Creative Commons Attribution 4.0 International License, which permits use, sharing, adaptation, distribution and reproduction in any medium or format, as long as you give appropriate credit to the original author(s) and the source, provide a link to the Creative Commons license, and indicate if changes were made. The images or other third party material in this article are included in the article’s Creative Commons license, unless indicated otherwise in a credit line to the material. If material is not included in the article’s Creative Commons license and your intended use is not permitted by statutory regulation or exceeds the permitted use, you will need to obtain permission directly from the copyright holder. To view a copy of this license, visit <http://creativecommons.org/licenses/by/4.0/>.

© The Author(s) 2023